Journal of Advanced Research in Fluid Mechanics and Thermal Sciences

Journal homepage:
https://semarakilmu.com.my/journals/index.php/fluid_mechanics_thermal_sciences/index
ISSN: 2289-7879

Numerical Investigation of Squeezing Flow of Ternary Hybrid Nanofluid (Cu-Al_2O_3-TiO_2/H_2O) between Two Parallel Plates in a Porous Medium with Thermal Radiation and Heat Source/Sink

Hemant Agarwal[1,*], Shyamanta Chakraborty[2], Rupam Shankar Nath[1]

[1] Department of Mathematics, Gauhati University, Guwahati-781014, Assam, India
[2] UGC-HRDC, Gauhati University, Guwahati-781014, Assam, India

ARTICLE INFO

Article history:
Received 20 July 2024
Received in revised form 30 October 2024
Accepted 12 November 2024
Available online 30 November 2024

Keywords:
Thermal radiation; parallel plate; heat source; ternary hybrid nanofluid; Darcy porous medium; bvp4c; MHD

ABSTRACT

This work aims to investigate the influence of thermal radiation on the magnetohydrodynamics squeezing flow of water-based ternary hybrid nanofluids between two parallel plates in a Darcy porous medium. The nanoparticles Cu, Al_2O_3, and TiO_2 are dispersed in a base fluid H_2O, resulting in the creation of a ternary hybrid nanofluid $Cu - Al_2O_3 - TiO_2/H_2O$. This study examines the deformation of the lower plate as the upper one advances towards it. The numerical results are computed using the 3-stage Lobatto IIIa method, which is specially implemented by Bvp4c in MATLAB. The effects of various parameters are visually illustrated through graphs and quantitatively shown in tables. The velocity profile $f'(\eta)$ shows a decrease in pattern when the parameters S and λ on the upper plate and Da on the lower plate are increased. Conversely, it displays an increasing pattern with higher values of Sq and λ on the lower plate, as well as Da on the upper plate. The absolute skin friction of the ternary hybrid nanofluid is seen to be approximately 5% higher than that of the regular nanofluid at both lower and upper plates. The heat transmission rate of the ternary hybrid nanofluid is higher at the upper plate compared to the lower plate.

1. Introduction

Ternary hybrid nanofluids consist of three distinct kinds of nanoparticles dispersed in a base fluid. This paper describes a study on a ternary hybrid nanofluid consisting of copper (Cu), aluminum oxide (Al_2O_3), and titanium dioxide (TiO_2) nanoparticles, which are uniformly dispersed in a water-based fluid. This ternary hybrid nanofluid possesses distinctive characteristics that enable it suited for a many different kinds of applications. Introducing copper (Cu) nanoparticles into the nanofluid has been discovered to enhance thermal conductivity, while the inclusion of aluminum oxide (Al_2O_3) and titanium dioxide (TiO_2) nanoparticles has been reported to improve heat transfer efficiency and stability. This nanofluid can be used in a range of applications, including heat exchangers, cooling systems, and electronic devices, to improve heat dissipation and enhance thermal management.

* *Corresponding author.*
E-mail address: hemantagarwal55@gmail.com

https://doi.org/10.37934/arfmts.124.2.90109

Copper nanoparticles exhibit antibacterial properties, while (TiO_2) nanoparticles demonstrate photocatalytic activity against bacteria and other microorganisms. The utilization of the ternary hybrid nanofluid, consisting of $Cu - Al_2O_3 - TiO_2$, has great potential for creating antibacterial coatings on different surfaces, such as textiles, medical equipment, and food packaging. These coatings efficiently hinder bacterial proliferation and help maintain hygiene. Titanium dioxide (TiO_2) nanoparticles possess photocatalytic characteristics, enabling them to effectively catalyze the decomposition of organic pollutants and the sterilization of water. The utilization of the $Cu - Al_2O_3 - TiO_2$, ternary hybrid nanofluid shows promise for implementation in water treatment processes, aiding in the removal of contaminants and improving the overall water quality.

Choi and Eastman [1] were the innovators who first introduced the concept of nanofluids. They claimed that by suspending metallic nanoparticles in conventional heat transfer fluids, a groundbreaking kind of heat transmission fluids might be created. Raees *et al.,* [2] has conducted an investigation of the unsteady squeezing flow of fluid between parallel plates that contains both nanoparticles and gyrotactic microorganisms, one of the plates was moving and the other staying still. Hayat *et al.,* [3] applied the HAM approach to study the magnetohydrodynamic squeezing flow of a nanofluid across a porous stretched surface with thermophoresis effects and Brownian motion. They have taken the lower wall of the channel to be permeable and stretched, while the upper impermeable wall moves in the direction of the lower wall at a prescribed time-dependent velocity. Moreover, Hayat *et al.,* [4] discovered a novel analysis of the magnetohydrodynamic squeezing flow of couple stress nanomaterial between two parallel surfaces. This analysis incorporates the unique characteristics of thermophoresis and Brownian motion, which have not been previously described together with a porous lower surface in the channel. Salehi *et al.,* [5] has conducted research on the magnetohydrodynamic squeezing nanofluid flow of hybrid nanoparticles composed of Fe_3O_4 and MoS_2 that are sandwiched between two infinite parallel plates. They found that as the squeezing and Hartman numbers increased, the velocity profile decreased. Acharya [6] performed research to determine the flow patterns and heat transmission characteristics of hybrid nano liquids in the presence of nonlinear solar radiation. The investigation focused on several solar thermal devices that had Alumina-copper nano ingredients mixed with water as the main fluid. Furthermore, Bio-convective nano liquid flow including gyrotactic microorganisms between two squeezed parallel plates was investigated by Acharya *et al.,* [7] using the classical Runge-Kutta-Fehlberg approach, taking into account the effects of a higher-order chemical reaction and second-order slip. Based on their research, they discovered that the temperature reduces as the squeezing factor and first-order velocity slip parameter increase, but increases as the second-order slip parameter increases. A micro-polar hybrid nanofluid ($GO - Cu/H_20$) has been investigated by Islam *et al.,* [8] in the presence of hall current and thermal radiations to look at how it moves and transfers heat between two surfaces in a spinning system. The primary result of their investigation is that increasing the values of the magnetic parameter leads to an increase in the velocity profile and a decrease in the rotational velocity profile. Also, the fractional model of Brinkman type fluid that contains hybrid nanoparticles of TiO_2 and Ag in a base fluid of water within a confined micro-channel has been investigated by Ikram *et al.,* [9]. Khashi'ie *et al.,* [10] investigated the $Cu - Al_2O_3/H_20$ nanofluid flow between two parallel plates in which a magnetic field and wall mass suction or injection are supplied to the lower plate, allowing the bottom plate to be deformed while the upper plate flows in the opposite direction of the lower plate. The primary finding of their investigation is that an augmentation in the squeezing parameter leads to a degradation of the heat transfer coefficient by 4.28% (upper) and 5.35% (lower), respectively. Yaseen *et al.,* [11] studied the heat transfer properties of the MHD squeezing nanofluid (MoS_2/H_2O) flow and the hybrid nanofluid ($MoS_2 - SiO_2/H_2O - C_2H_6O_2$) flow between two parallel plates, as well as their symmetrical characteristics. In their model, the upper plate is

moving downwards towards the lower plate, while the bottom plate is elongating with a constant velocity. A hybrid nanofluid containing Ethylene glycol-water as the base fluid and nanoparticles of TiO_2 and MoS_2 in the presence of dust particles and a magnetic field, flowing over a stretched sheet, was studied by Rostami *et al.,* [12] in terms of its motion and temperature distribution in a porous medium. By considering the effects of thermal radiation and Hall current, Rauf *et al.,* [13] investigated the micropolar tri-hybrid nanofluid($Fe_3O_4 - Al_2O_3 - TiO_2/H_2O$) in a rotating structure between two perpendicular permeable plates. A micro-polar fluid undergoing radiative and magnetohydrodynamic flow across an Al_2O_3 and Cu nanoparticle stretched/shrinking sheet in the presence of viscous dissipation and Joule heating was investigated by Waini *et al.,* [14]. Famakinwa *et al.,* [15] studied how heat radiation and viscous dissipation affect an unstable, incompressible flow of water-hybrid nanoparticles moving between two surfaces that are lined up and have different viscosity. They discovered that there was no apparent alteration in fluid velocity when thermal radiation and viscous dissipation parameters were increased, but that the temperature distribution was reduced. The combined effects of the suction/injection, electromagnetic force, activation energy, chemical reaction, ionized fluid, inertia force and magnetic field that influence the squeezing flow of ternary hybrid nanofluids between parallel plates are investigated numerically by Bilal *et al.,* [16]. Hanif *et al.,* [17] investigated the flow of a hybrid nanofluid based on an aluminum alloy and water across a stretchy horizontal plate with a thermal resistive effect using the Numerical Crank-Nicolson approach. The MHD flow, heat, and mass transfer of the Jeffrey hybrid nanofluid on the squeezing channel via a permeable material in the presence of a chemical reaction and a heat sink/source were studied by Noor and Shafie [18]. Ullah *et al.,* [19] explored the hydrothermal properties of a hybrid nanofluid $(Ag + TiO_2 + H_2O)$ in three dimensions in presence of magnetic, thermal, and radiation fluxes between the two vertical plates. Transient free convection of a hybrid nanofluid between two parallel plates in the presence of a magnetic field, a heat source/sink and thermal radiation was explored analytically by Roy and Pop [20]. Moreover, the effect of radiative heat flux on the transient state electro-osmotic squeezing propulsion of a viscous liquid via a porous material between two parallel plates has been investigated by Jayavel *et al.,* [21]. Bhaskar *et al.,* [22] and Maiti and Mukhopadhyay [23] investigated the MHD squeezed flow of casson hybrid nanofluid and unstable nanofluid flow between two parallel plates, respectively, under various effects. Madit *et al.,* [24] studied how a chemical reaction affects the flow of a nanofluid that is squeezed by hydro magnetism between two vertical plates. Khashi'ie *et al.,* [25] carried out investigations into the simultaneous impact of double stratification and buoyancy forces on the flow of nanofluid over a surface that is either shrinking or stretching. It was observed that the heat transfer rate increases by roughly 5.83% to 12.13% when the thermal relaxation parameter is introduced in both shrinking and stretching scenarios. Similarly, Khashi'ie *et al.,* [26] developed numerical solutions and conducts stability analyses for stagnation point flow utilizing hybrid nanofluid in the presence of thermal stratification across a permeable stretching/shrinking cylinder. Nath and Deka [27] studied the effects of thermal and mass stratification on an unsteady MHD nanofluid past a vertical plate that accelerates exponentially with temperature variation in a porous media. Similarly, Nath and Deka [28] conducted a numerical study to examine the combined impacts of thermal and mass stratification on the movement of unstable magnetohydrodynamic nanofluid through an exponentially accelerated vertical plate in a porous media. The unsteady parabolic flow across an infinite vertical plate with exponentially declining temperature and variable mass diffusion in a porous media has been investigated by Nath and Deka [29] with respect to the thermal and mass stratification effect. Nath and Deka [30,31] performed a numerical investigation on the MHD ternary hybrid nanofluid around a vertically stretching cylinder in a porous medium with thermal stratification.

Using artificial neural networks and the Levenberg–Marquardt backpropagation method, Ullah *et al.,* [32] looked at how electric and magnetic fields affected the flow of a micro-polar nano-fluid between two parallel plates that were rotating. Ullah *et al.,* [33], Shoaib *et al.,* [34] and Akbar *et al.,* [35] investigated the micropolar flow, Maxwell Nanofluid Flow and two phase model of nano-fluid flow using the Levenberg–Marquardt back propagation with neural networks (TLMB-NN) technique, under various conditions. Similarly, Akbar *et al.,* [36] uses the Levenberg Marquardt back-propagation neural networks scheme to analyze the Buongiorno model of the MHD nano-fluid flow through a rotating disc with partial slip effects. Ullah *et al.,* [37] obtained the analytical solution for the three-dimensional problem of condensation film on an inclined rotating disc using the extended optimal homotopy asymptotic method. Fiza *et al.,* [38] conducted a study on the behavior of a viscoelastic second-grade nano liquid with heat transmission between two parallel plates in a rotating system, specifically focusing on magnetohydrodynamics (MHD). Elfiano *et al.,* [39] investigated the flow and heat transmission characteristics of a hybrid nanofluid $(Al_20_3 - Ag/H_2O)$ on a vertical flat plate with different volume concentrations and the inclusion of viscous dissipation effects. Annapurna *et al.,* [40] conducted a study on the impact of various nanoparticle shapes on the flow of mixed convective nanofluid in a porous medium using the Darcy-Forchhiemer model.

Based on the literature review, previous research has not attempted to investigate the squeezing flow of an MHD ternary hybrid nanofluid between two parallel plates in a porous media. It is assumed that the lower plate has a physically permeable and stretchable shape. The primary aim of this study is to investigate the thermal conductivity characteristics of a ternary hybrid nanofluid composed of $Cu - Al_2O_3 - TiO_2$ particles suspended in water. This study examines the heat transfer characteristics between two parallel plates, considering the influence of thermal radiation as well as heat sources/sinks. The bvp4c solver in MATLAB is used to transform the non-linear PDEs into ODEs by utilizing the necessary self-similarity variables. The Bvp4c technique employed in this research work to represent the problem is generally acknowledged, as evidenced by its discussion and implementation in MATLAB by Hale and Moore [41]. A visual depiction of the outcomes is presented for many parameters, including $\delta, Sq, S, \lambda, M, Da, R$ and Q.

2. Methodology

Let us consider a two-dimensional unsteady ternary hybrid nanofluid $(Cu - Al_2O_3 - TiO_2/H_2O)$ squeezing flow between two infinite parallel plates in a Darcy porous medium, as presented in Figure 1.

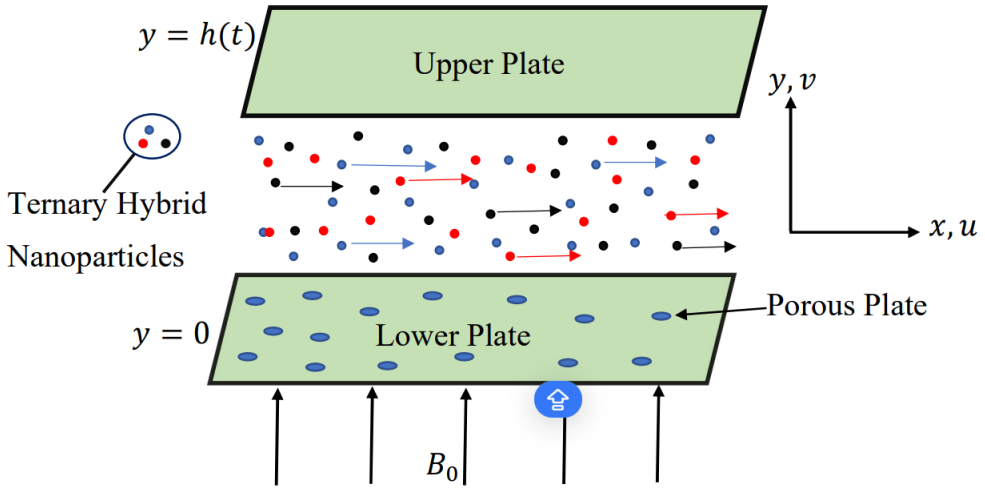

Fig. 1. Physical Model and Coordinate System

The upper plate is positioned at a distance of $y = h(t) = \sqrt{\frac{(1-\alpha t)\upsilon_f}{b}}$ from the lower plate. At the same time, the higher plate, with a velocity $V_h = \frac{dh(t)}{dt} = -\frac{\alpha}{2}\sqrt{\frac{\nu_f}{(1-\alpha t)b}}$ is moving towards the lower plate that is being squeezed. It is presumed that the lower and upper plates are kept at constant temperatures T_1 and T_2, respectively. Additionally, the influence of thermal radiation and heat source/sink are taken into consideration in this model; however, the buoyancy effect, which is also known as the gravitational force, is not taken into account. In the meantime, the physical representation for the potential fluid suction or injection includes the porous lower plate, where the wall mass velocity is represented as $v_w = -\frac{V_0}{1-\alpha t}$; for suction, $V_0 > 0$, for injection, $V_0 < 0$, and an impermeable plate corresponds to $V_0 = 0$. Furthermore, the lower plate can be stretched with a linear velocity of $u_w = -\frac{bx}{1-\alpha t}$, where $t < \frac{1}{\alpha}$, and a time-dependent magnetic field is modeled with $B(t) = \frac{B_0}{1-\alpha t}$. In light of these assumptions and with the hybrid nanofluid model that Khashi'ie *et al.,* [10] and Yaseen *et al.,* [11] have proposed, we extended their model to incorporate the ternary hybrid model. Hence, the governing conservation equations are as follows:

$$\frac{\partial u}{\partial x} + \frac{\partial v}{\partial y} = 0 \tag{1}$$

$$\frac{\partial V}{\partial t} + u\frac{\partial V}{\partial x} + v\frac{\partial V}{\partial y} = \frac{\mu_{thnf}}{\rho_{thnf}}\frac{\partial^2 V}{\partial y^2} - \frac{\sigma_{thnf}}{\rho_{thnf}}B(t)^2 V - \frac{\mu_{thnf}}{\rho_{thnf}}\frac{\phi^* V}{k_p} \tag{2}$$

$$\frac{\partial T}{\partial t} + u\frac{\partial T}{\partial x} + v\frac{\partial T}{\partial y} = \frac{k_{thnf}}{(\rho c_p)_{thnf}}\frac{\partial^2 T}{\partial y^2} - \frac{1}{(\rho c_p)_{thnf}}\frac{\partial q_r}{\partial y} + \frac{Q_0}{(\rho c_p)_{thnf}}(T - T_0) \tag{3}$$

Where $V = \frac{\partial v}{\partial x} - \frac{\partial u}{\partial y}$. The boundary conditions that are associated with the lower and upper plates are as follows [3,10]:

$$u = \lambda\frac{bx}{1-\alpha t}, \quad v = -\frac{V_0}{1-\alpha t}, \quad T = T_1 \quad \text{at } y = 0 \text{ (lower plate)}$$

$$u = 0, \quad v = \frac{dh(t)}{dt}, \quad T = T_2 \quad \text{at } y = h(t) \text{ (upper plate)}$$

Here, u and v represent the velocities in the x and y directions, respectively, while T denotes the temperature of the ternary hybrid nanofluid. In addition, the other symbol signifies the following: ρ represents density, μ represents dynamic viscosity, Cp represents heat capacity, k represents thermal conductivity, $B(t)$ represents magnetic field strength, ϕ^* represents porosity of the porous medium, k_p represents permeability of the porous medium, λ represents the stretching/shrinking parameter, Q_0 represents heat absorption/generation coefficient, and b represents the stretching/shrinking rate of the lower plate.

Taking into consideration the Rosseland approximation, the value of (q_r) is defined as [42]

$$q_r = -\frac{4\sigma^*}{3k_{thnf}}\left(\frac{\partial T^4}{\partial y}\right)$$

The term "σ^*" represents the Stefan-Boltzmann constant, whereas "k_{thnf}" refers to the mean absorption coefficient. By performing basic calculations with the aforementioned term, Eq. (3) can be reduced as follows:

$$\frac{\partial T}{\partial t} + u\frac{\partial T}{\partial x} + v\frac{\partial T}{\partial y} = \frac{1}{(\rho c_p)_{thnf}}\left(k_{thnf} + \frac{16\sigma^* T_2^3}{3k}\right)\frac{\partial^2 T}{\partial y^2} + \frac{Q_0}{(\rho c_p)_{thnf}}(T - T_0)$$

The similarity transformation employed in Eq. (1) to Eq. (3) can be described as follows [3]:

$$u = \frac{bx}{1-\alpha t}f'(\eta),\ \ v = -\sqrt{\frac{b\,\upsilon_f}{1-\alpha t}}f'(\eta),\quad \eta = y\sqrt{\frac{b}{(1-\alpha t)\upsilon_f}},\quad \psi = \sqrt{\frac{b\upsilon_f}{1-\alpha t}}xf(\eta),\quad \theta = \frac{T-T_0}{T_2-T_0}$$

and we give non-dimensional quantities as follows:

$$M = \frac{B_0^2\sigma_f}{a\rho_f},\ Da = \frac{k_p b}{\upsilon_f(1-\alpha t)\phi^*},\ Sq = \frac{\alpha}{b},\ S = \frac{V_0}{hb},\ \delta = \frac{T_1-T_0}{T_2-T_0},\ Q = \frac{Q_0}{1-\alpha t},\ R = \frac{4\sigma^* T_2^3}{k_f k},\ Pr = \frac{(\rho c_p)_f}{k_f}$$

where, M is the magnetic parameter, Da is the Darcy number, Sq is the squeezing parameter, S is the suction/injection parameter, δ is the temperature-ratio parameter, Q is the heat source/sink parameter, R is the thermal radiation parameter, Pr is the Prandtl number. Moreover, if $\lambda = 0$, it means the lower plate is not moving, if $\lambda < 0$, it means the lower plate is shrinking, and if $\lambda > 0$, it means the lower plate stretching.

The non-dimensional types of the transformed equations are represented by

$$a_1 a_2 f'^v + ff''' - f'f'' - \frac{Sq}{2}(3f'' + \eta f''') - \left(a_2 a_3 M + \frac{a_1 a_2}{Da}\right)f'' = 0 \tag{4}$$

$$\frac{a_4}{Pr}\left(a_5 + \frac{4}{3}R\right)\theta'' + f\theta' - \frac{Sq}{2}\eta\theta' + a_4 Q\theta = 0 \tag{5}$$

where,

$$a_1 = \frac{\mu_{thnf}}{\mu_f},\ a_2 = \frac{\rho_f}{\rho_{thnf}},\ a_3 = \frac{\sigma_{thnf}}{\sigma_f},\ a_4 = \frac{(\rho c_p)_f}{(\rho c_p)_{thnf}},\ a_5 = \frac{k_{thnf}}{k_f}$$

Here, the symbols $\mu_{thnf}, \rho_{thnf}, \sigma_{thnf}, (\rho c_p)_{thnf}, k_{thnf}$ refers to the ternary hybrid nanofluid's coefficient of viscosity, density, electrical conductivity, heat capacity and thermal conductivity, respectively. Also, $\mu_f, \rho_f, \sigma_f, (\rho c_p)_f, k_f$ represents the base fluid's coefficient of viscosity, density, electrical conductivity, heat capacity and thermal conductivity correspondingly.

The boundary conditions that have been transformed are as such:

$$f(0) = S, \quad f'(0) = \lambda, \quad \theta(0) = \delta$$

$$f(1) = \frac{Sq}{2}, \quad f'(1) = 0, \quad \theta(1) = 1$$

where ϕ_1, ϕ_2, ϕ_3 are volume fraction of *Cu* (Copper), Al_2O_3(aluminium oxide) and TiO_2 (titanium oxide) nanoparticles correspondingly. The suffixes *thnf, hnf, nf, f, s1, s2, s3* refers to the ternary hybrid nanofluid, hybrid nanofluid, nanofluid, base fluid, solid nanoparticles of copper *(Cu),* aluminum oxide (Al_2O_3), and titanium dioxide (TiO_2) correspondingly. The thermophysical characteristics of the ternary hybrid nanofluid are presented in Table 1. Thermo-physical properties of Cu, Al_2O_3 and TiO_2 nanoparticles in pure water are given in Table 2.

The skin friction coefficient and local Nusselt number are defined as follows

Lower: $C_{f_1} Re_x^{1/2} = \frac{\mu_{thnf}}{\mu_f} f''(0)$ and Upper: $C_{f_2} Re_x^{1/2} = \frac{\mu_{thnf}}{\mu_f} f''(1)$

Lower: $Nu_{x_1} Re_x^{-1/2} = -\left(\frac{k_{thnf}}{k_f} + \frac{4}{3}R\right)\theta'(0)$ and Upper: $Nu_{x_2} Re_x^{-1/2} = -\left(\frac{k_{thnf}}{k_f} + \frac{4}{3}R\right)\theta'(1)$

where, $Re_x \frac{xU_w}{\upsilon_f}$ is the local Reynolds Number.

Table 1
The thermophysical properties of ternary hybrid nanofluid are given by [30]

Properties	Ternary Hybrid Nanofluid
Dynamic Viscosity (μ)	$\frac{\mu_{thnf}}{\mu_f} = \frac{1}{(1-\phi_1)^{2.5}(1-\phi_2)^{2.5}(1-\phi_3)^{2.5}}$
Density (ρ)	$\rho_{thnf} = (1-\phi_3)\left[(1-\phi_2)\left\{(1-\phi_1)\rho_f + \phi_1\rho_{s1}\right\} + \phi_2\rho_{s2}\right] + \phi_3\rho_{s3}$
Electrical Conductivity (σ)	$\sigma_{thnf} = \left[\frac{(\sigma_{s2} + 2\sigma_{hnf}) - 2\phi_2(\sigma_{hnf} - \sigma_{s2})}{(\sigma_{s1} + 2\sigma_{hnf}) + \phi_2(\sigma_{hnf} - \sigma_{s2})}\right]\sigma_{hnf}$
	$\sigma_{hnf} = \left[\frac{(\sigma_{s2} + 2\sigma_{nf}) - 2\phi_2(\sigma_{nf} - \sigma_{s2})}{(\sigma_{s1} + 2\sigma_{nf}) + \phi_2(\sigma_{nf} - \sigma_{s2})}\right]\sigma_{nf}$
	$\sigma_{nf} = \left[\frac{(\sigma_{s1} + 2\sigma_f) - 2\phi_1(\sigma_f - \sigma_{s1})}{(\sigma_{s1} + 2\sigma_f) + \phi_1(\sigma_f - \sigma_{s1})}\right]\sigma_f$
Heat Capacity (ρC_p)	$(\rho c_p)_{thnf} = (1-\phi_3)\left[(1-\phi_2)\left\{(1-\phi_1)(\rho c_p)_f + \phi_1(\rho c_p)_{s1}\right\} + \phi_2(\rho c_p)_{s2}\right] + \phi_3(\rho c_p)_{s3}$
Thermal Conductivity (k)	$k_{thnf} = \left[\frac{(k_{s3} + 2k_{hnf}) - 2\phi_3(k_{hnf} - k_{s3})}{(k_{s3} + 2k_{hnf}) + \phi_3(k_{hnf} - k_{s3})}\right]k_{hnf}$
	$k_{hnf} = \left[\frac{(k_{s2} + 2k_{nf}) - 2\phi_2(k_{nf} - k_{s2})}{(k_{s2} + 2k_{nf}) + \phi_2(k_{nf} - k_{s2})}\right]k_{nf}$
	$k_{nf} = \left[\frac{(k_{s1} + 2k_f) - 2\phi_1(k_f - k_{s1})}{(k_{s1} + 2k_f) + \phi_1(k_f - k_{s1})}\right]k_f$

Table 2
Thermo-physical properties of water and nanoparticles [43]

Thermophysical Properties	H_2O (base fluid)	Cu (s1)	Al_2O_3 (s2)	TiO_2 (s3)
$\rho\ (Kg/m^3)$	997.1	8933	3970	4250
$c_p\ (J/KgK)$	4179	385	765	686.2
$k\ (W/mK)$	0.613	401	40	8.9538
$\sigma\ (s/m)$	5.5×10^{-6}	59.6×10^{6}	35×10^{6}	2.6×10^{6}

3. Method of Solution

In order to obtain numerical solutions for a system of higher-order nonlinear ordinary differential equations (ODEs) provided by Eq. (4) and Eq. (5) and the boundary conditions, we use the bvp4c solver, built into the computational platform MATLAB. Professionals and researchers have widely employed this technique for solving fluid flow problems. The bvp4c solver, developed by Jacek Kierzenka and Lawrence F. Shampine from Southern Methodist University in Texas, was first presented by Hale and Moore [41]. The bvp4c solver is an algorithm that employs the Lobato IIIA implicit Runge-Kutta technique to provide numerical solutions with fourth-order accuracy. It achieves this by making finite modifications. This method provides the required precision when an estimation is made for the initial mesh points and adjustments to the step size. The investigation conducted by Waini *et al.,* [44] shown that the bvp4c solver produced satisfactory outcomes when compared to both the direct shooting approach and Keller box method. The syntax for using the "bvp4c" solver is as follows: "sol = bvp4c (@OdeBVP, @OdeBC, solinit, options)". Here, we must decrease the higher order derivatives in relation to η. This can be accomplished by introducing the subsequent new variables:

$$f = y(1),\ f' = y(2),\ f'' = y(3),\ f''' = y(4),\ \theta = y(5),\ \theta' = y(6)$$

$$\frac{d}{d\eta}\begin{bmatrix} y(1) \\ y(2) \\ y(3) \\ y(4) \\ y(5) \\ y(6) \end{bmatrix} = \begin{bmatrix} y(2) \\ y(3) \\ y(4) \\ \dfrac{y(2)y(3) - y(1)y(4) + \frac{Sq}{2}\left(3y(3) + \eta y(4)\right) + \left(a_2 a_3 M + \frac{a_1 a_2}{Da}\right) y(3)}{a_1 a_2} \\ y(6) \\ \dfrac{\frac{Sq}{2}\eta y(6) - a_4 Q y(5) - y(1)y(6)}{\frac{a_4}{Pr}\left(a_5 + \frac{4}{3}R\right)} \end{bmatrix}$$

and boundary condition are written as

$$y_0(1) - S,\ y_0(2) - \lambda,\ y_0(5) - \delta,\ y_1(1) - \frac{Sq}{2},\ y_1(2),\ y_1(5) - 1$$

Where y_0 is the condition at $\eta = 0$ and $y_1$is the condition at $\eta = 1$.

4. Results and Discussion

The results are computed by using bvp4c in MATLAB and visually displayed in Figure 2 to Figure 14 for the distribution of skin friction coefficients, velocity, local Nusselt number and temperature on both the upper and bottom plates. The Prandtl number is set at a constant value of 6.2, indicating

the utilization of water at a temperature of $25°C$. The other parameters are constrained within the following ranges: $0 \leq \delta \leq 0.3$ for the temperature-ratio parameter, $0 \leq Sq \leq 1.5$ for the unsteadiness squeezing parameter, $-1.2 \leq S \leq 1.2$ for the suction/injection parameter, $-0.5 \leq \lambda \leq 2$ for the stretching/shrinking parameter, $0 \leq Da \leq 0.1$ for the porous medium parameter and $0 \leq M \leq 5$ for the magnetic parameter, $0 \leq R \leq 3$ for the thermal radiation parameter, $-0.2 \leq Q \leq 0.2$ for the heat source/sink parameter. The comparison of $f''(1)$ for the upper plate with Hayat *et al.,* [3] and Khashi'ie *et al.,* [10] for varying values of M, S, Sq when $\lambda = 1, \phi_1 = \phi_2 = \phi_3 = 0$ is presented in Table 3. It can be seen that the results of this study are very similar to those of the two prior investigations, which validates codes of our method and the results of this study.

Table 3
Comparison of $f''(1)$ for upper plate when $\lambda = 1, \phi_1 = \phi_2 = \phi_3 = 0$

M	S	Sq	Hayat *et al.,* [3] $f''(1)$	Khashi'ie *et al.,* [10] $f''(1)$	Present Study $f''(1)$
0.25	0.5	1	1.80818	1.80817	1.80817
0.25	0.5	1.5	0.28395	0.28394	0.28394
0.25	1	1	4.57302	4.57301	4.57301
1	0.5	1	1.78937	1.78937	1.78937

The parameters were set at fixed values for the computation of the results: $\delta = 0.1, Sq = 1.5, M = 1.5, Da = 0.05, S = 0.3, \lambda = 1, R = 1, Q = 0.2, \phi_1 = \phi_2 = \phi_3 = 0.01$. Figure 2 displays the impact of Darcy number (Da) on velocity profile $f'(\eta)$ of the ternary hybrid nanofluid. In close proximity to the lower plate, the velocity experiences a sudden increase as the Darcy number increases. However, there is a distinct transition point at $\eta \sim 0.4$, beyond which the velocity exhibits contrasting behavior. The Darcy number (Da) determines the ratio of the permeability of a medium to its cross-sectional area, while permeability measures the ability of a surface to allow fluid to pass through its membrane. The rising permeability in the surrounding area of the bottom plate hinders the movement of the fluid. Consequently, a rise in the Darcy number (Da) results in velocity profiles that are closer to the upper plate due to greater flow resistance. The influence of the magnetic parameter(M) on the velocity profile is depicted in Figure 3. The velocity of the ternary hybrid nanofluid reduces as the magnetic parameter increases when it is in close proximity to the lower plate. Just like Figure 2, Figure 3 also shows a transition point around $\eta \sim 0.4$. After reaching this transition point, the velocity demonstrates contrasting behavior. A strong magnetic field leads to a substantial decrease in the mobility of liquids. With an increase in the magnetic field strength(M), the Lorentz forces come into play and result in a reduction in the liquid flow. A magnetic field impedes the movement and ultimately reduces the radial velocity.

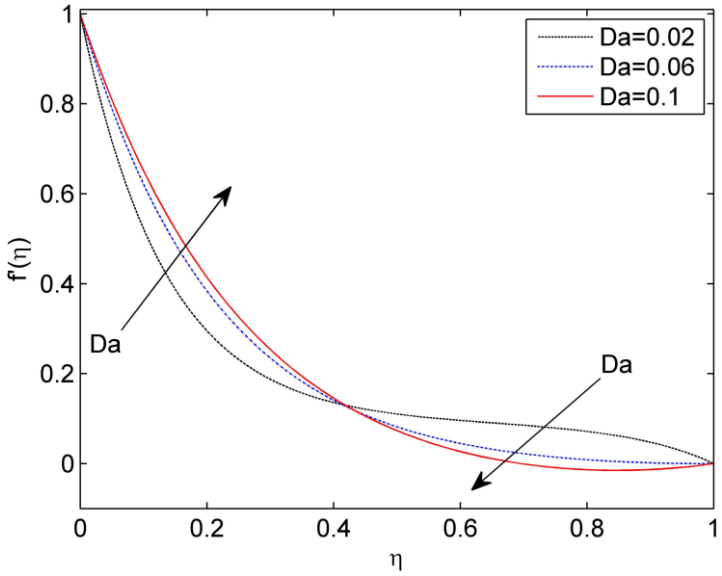

Fig. 2. Effect of Da on $f'(\eta)$

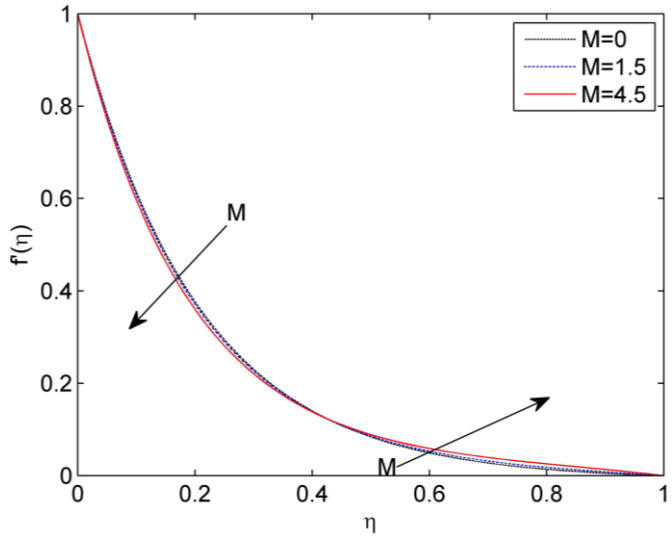

Fig. 3. Effect of M on $f'(\eta)$

As seen in Figure 4, the addition of the unsteadiness squeezing parameter (Sq) improves the velocity distribution $f'(\eta)$ for the ternary hybrid nanofluid. Due to the movement of the upper plate towards the lower plate, the squeezing effect is initiated from the higher plate. It has been observed that the velocity of the fluid increases in tandem with the squeezing parameter (Sq) as it rises higher. Figure 5 illustrates the effect of the suction/injection parameter (S) on the velocity profile $f'(\eta)$. As seen in the figure, the application of injection results in a higher velocity than suction. Suction/injection is frequently employed as a means to prevent boundary layer separation. In this study, the application of injection results in an observed enhancement in velocity. Therefore, in this study, the injection is more efficient in delaying the separation of the boundary layer. Figure 6 demonstrates the impact of the shrinking/stretching parameter(λ) on the velocity profile $f'(\eta)$ for the ternary hybrid nanofluid. The velocity profile $f'(\eta)$ exhibits dual behavior with respect to shrinking/stretching parameter(λ). There is a transition point located close to $\eta \sim 0.3$. The velocity $f'(\eta)$, increases in the surrounding area of the lower plate, but beyond the transition point, the velocity $f'(\eta)$, declines. This outcome suggests that the stretching of the lower plate increases velocity in the surrounding area of the lower plate. However, when the upper plate moves towards

the lower plate, the velocity behaves in the opposite way when the parameter(λ) increases. The impact of the temperature-ratio parameter (δ) on the temperature profile $\theta(\eta)$ is shown in Figure 7. The temperature-ratio parameter (δ) is found to increase the temperature of the ternary hybrid nanofluid due to obvious and expected reasons.

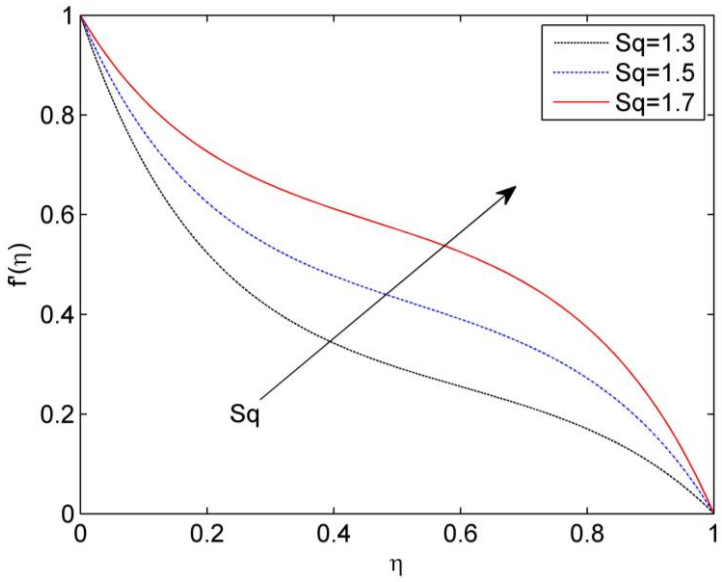

Fig. 4. Effect of Sq on $f'(\eta)$

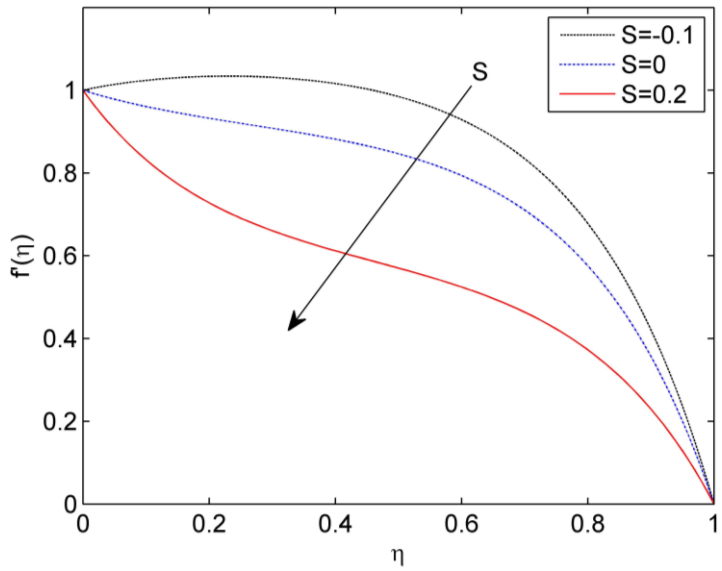

Fig. 5. Effect of S on $f'(\eta)$

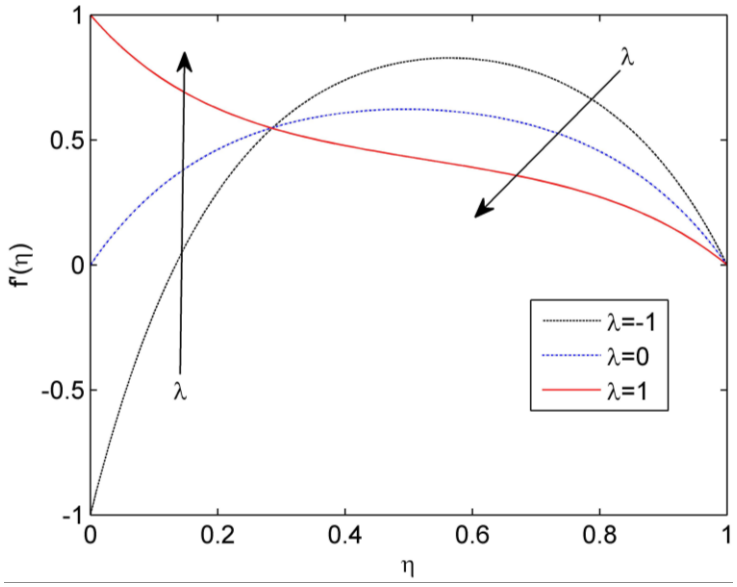

Fig. 6. Effect of $\boldsymbol{\lambda}$ on $\boldsymbol{f'(\eta)}$

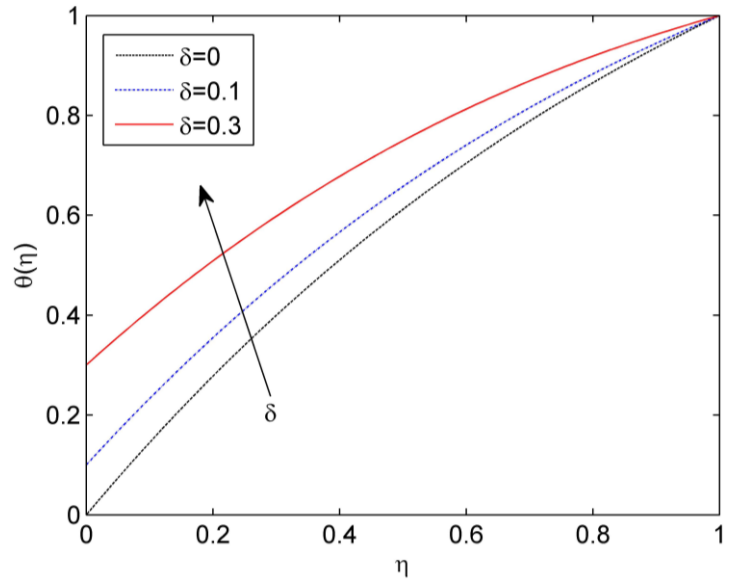

Fig. 7. Effects of δ on $\theta(\eta)$

Figure 8 displays that the temperature $\theta(\eta)$ of the ternary hybrid nanofluid goes down as the thermal radiation (R) goes up. Thermal radiation causes the temperature of the nanofluid to decrease by causing a net loss of energy from the fluid. This loss of energy reduces the kinetic energy of the particles inside the fluid, leading to a lower temperature. Figure 9 demonstrates the increasing effects of temperature as the heat generation/absorption parameter (Q) increases. Greater values of a parameter (Q) result in an increase in temperature. The parameter (Q) has positive values, indicating the production of heat in the system. Higher values of (Q) correspond to greater amounts of heat being generated. Therefore, as the heat-generation parameter (Q) increases, the temperature also increases. Figure 10 demonstrates the influence of the squeezing parameter (Sq) on the temperature profile $\theta(\eta)$. It is easy to see from the graph that as the squeezing parameter (Sq) goes up, the temperature goes down. This indicates that when the upper plate moves closer to the lower plates, it limits the spread of heat, resulting in a fall in temperature.

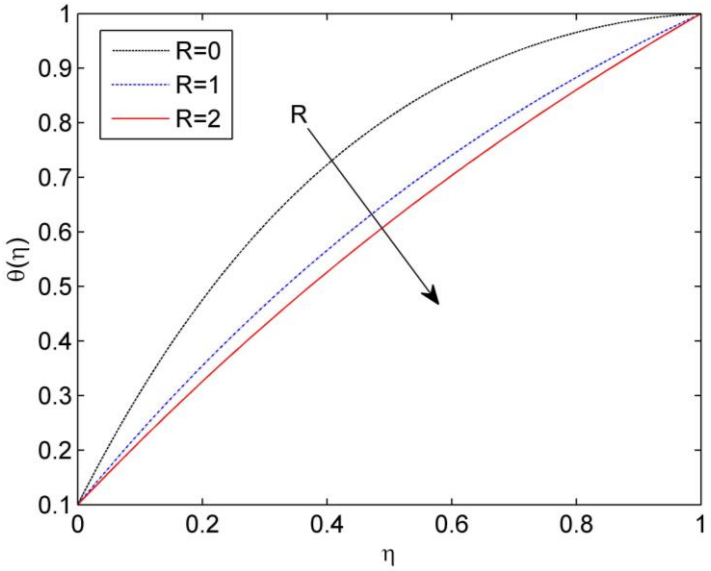

Fig. 8. Effect of R on $\theta(\eta)$

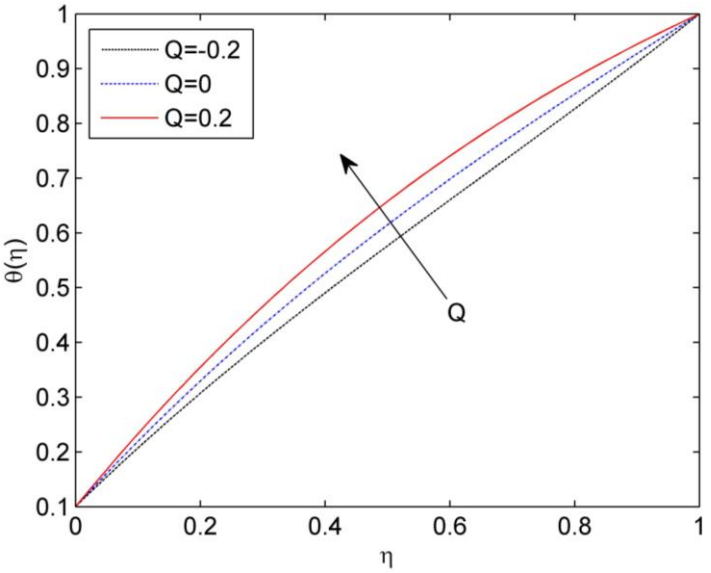

Fig. 9. Effect of $\boldsymbol{Q}$ on $\boldsymbol{\theta(\eta)}$

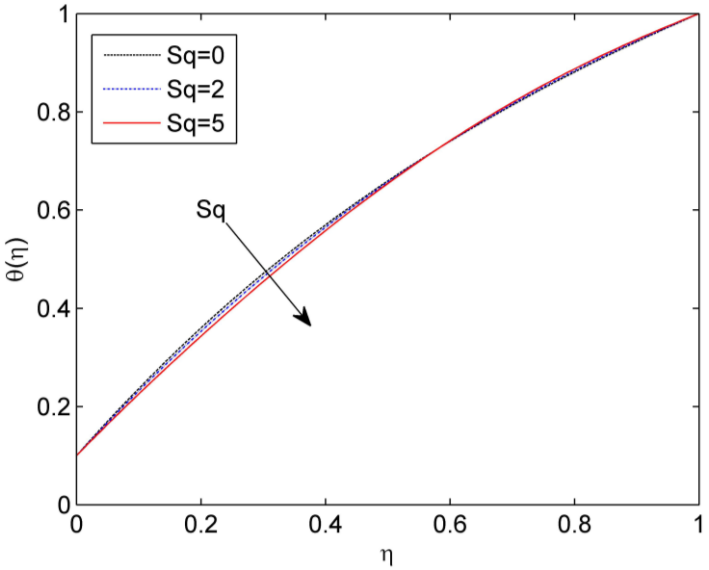

Fig. 10. Effects of Sq on $\theta(\eta)$

Figure 11 illustrates the fluctuation of the temperature, $\theta(\eta)$ for ternary hybrid nanofluid, in response to changes in the suction/injection parameter (S). An increase in parameter (S) leads to an observed rise in θ(η). The temperature is observed to be higher for the suction value as compared to the injection value. Suction refers to the process of extracting the layers that are detached from the border layer using suction. The fluid layers experience an increase in temperature as they gain momentum through the use of suction. The influence of the stretching/shrinking parameter(λ) on the temperature $\theta(\eta)$ is demonstrated in Figure 12. This model says that $\lambda = 0$ means the lower plate is still, $\lambda < 0$ means it is shrinking, and $\lambda > 0$ means it is stretching. It is observed that the velocity, $f'(\eta)$, increases as the values of (λ) increase. The findings suggest that the stretching of the lower plate increases the temperature of the flow. In addition, when the degree of shrinkage of the lower plate increases, the temperature decreases.

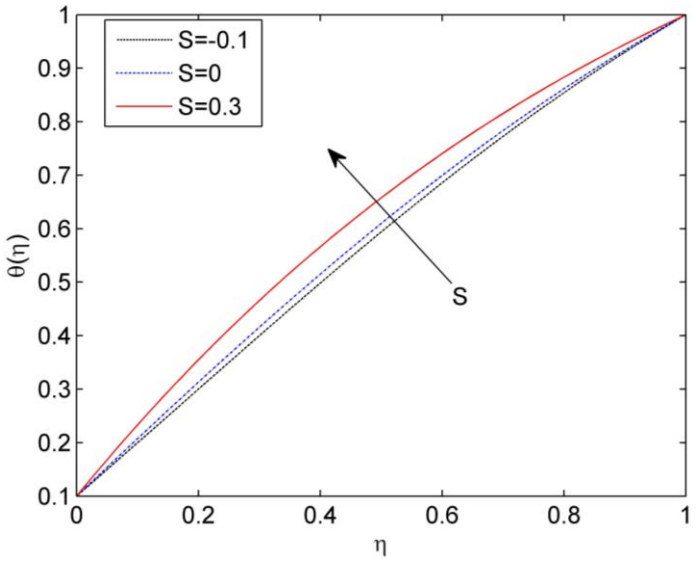

Fig. 11. Effect of S on $\theta(\eta)$

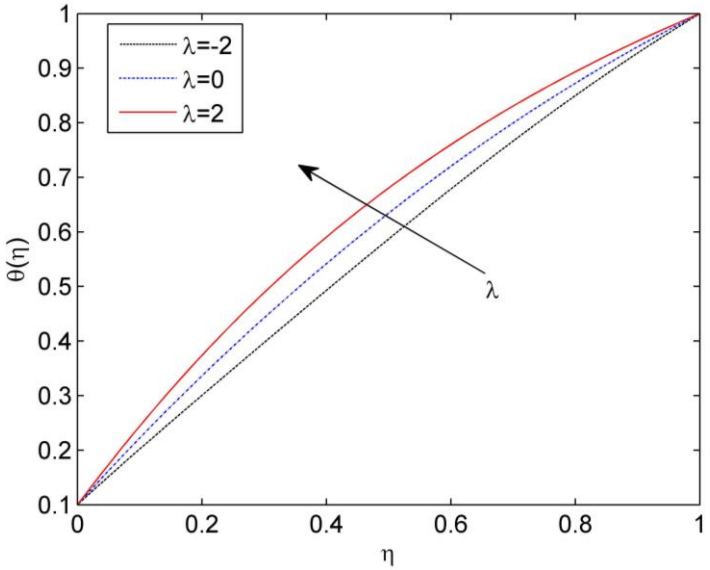

Fig. 12. Effect of λ on $\theta(\eta)$

Table 4 presents the values of the skin friction coefficients $C_{f_1}Re_x^{1/2}$ and $C_{f_2}Re_x^{1/2}$, as well as the Nusselt numbers $Re_x^{-1/2}Nu_{x_1}$ and $Re_x^{-1/2}Nu_{x_1}$, for various combinations of parameters at the lower and upper plate. The Nusselt numbers express the rates of heat transmission between the upper and bottom plates. An increase in the temperature ratio parameter(δ) leads to a rise in the Nusselt number for both the lower and higher plates. The skin friction coefficient is not influenced by temperature ratio parameter(δ), radiation (R), and heat source (Q) at both plates, as these physical factors are independent of the velocity profile $f'(\eta)$.

Table 4
Skin friction Coefficient and Nusselt number for various values of $\delta, Sq, M, Da, S, \lambda, R, Q$

δ	Sq	M	Da	S	λ	R	Q	$Re_x^{1/2}C_{f_1}$	$Re_x^{1/2}C_{f_2}$	$Re_x^{-1/2}Nu_{x_1}$	$Re_x^{-1/2}Nu_{x_2}$
0.1	1.5	1.5	0.05	0.3	1	1	0.2	-3.2027	-2.2578	-3.3528	-1.2784
0.3								-3.2027	-2.2578	-2.7742	-0.8530
0.1	0.5	1.5	0.05	0.3	1	1	0.2	-7.5185	2.0476	-3.4166	-1.3022
	1							-5.3795	-0.0861	-3.3844	-1.2902
0.1	1.5	0.5	0.05	0.3	1	1	0.2	-3.1452	-2.2094	-3.3549	-1.2769
		1						-3.1740	-2.2337	-3.3538	-1.2777
0.1	1.5	1.5	0.08	0.3	1	1	0.2	-2.7530	-1.8795	-3.3706	-1.2661
			0.1					-2.5888	-1.7410	-3.3776	-1.2614
0.1	1.5	1.5	0.05	0.5	1	1	0.2	-5.0506	-0.5500	-3.9324	-1.1084
				-0.2				1.2148	-6.6393	-2.1855	-1.7193
0.1	1.5	1.5	0.05	0.3	0.5	1	0.2	0.4190	-3.0652	-3.2113	-1.3430
					-0.5			7.5525	-4.7130	-2.9369	-1.4760
0.1	1.5	1.5	0.05	0.3	1	2	0.2	-3.2027	-2.2578	-4.4777	-2.4856
						3		-3.2027	-2.2578	-5.6436	-3.6892
0.1	1.5	1.5	0.05	0.3	1	1	0	-3.2027	-2.2578	-2.9992	-1.7515
							-0.2	-3.2027	-2.2578	-2.6845	-2.1908

Increasing the squeezing parameter (Sq) enhances the heat transfer rate at the both plates. However, it reduces the skin friction coefficient at the upper plate and increases it at the lower plate. The magnetic parameter(M) causes a drop in the skin friction coefficient on both the lower and upper plates. However, it leads to an increase in the Nusselt number on the lower plate and a decrease on the upper plate. Observations indicate that a rise in the Darcy number(Da) leads to an

increase in the skin friction coefficient on both the upper and lower plates. Nevertheless, it results in a decrease in the Nusselt number on the lower plate and an increase on the upper plate. The suction/injection(S) parameter reduces the skin friction coefficient on the bottom plate, but raises it on the top plate. Similarly, the rate of heat transmission reduces at the bottom plate but increases at the top plate. The skin friction coefficient at the lower plate increases as the stretching parameter(λ) is increased, whereas it decreases at the higher plate. Similarly, the rate of heat transmission increases at the bottom plate while it decreases at the top plate. Radiation(R), causes a drop in the Nusselt number at both the lower and upper plates, while the heat source(Q) results in a fall in the Nusselt number at the lower plate and an increase at the upper plate.

Table 5 and Table 6 present an analysis of the percentage difference between the nanofluid with hybrid nanofluid and ternary hybrid nanofluid in terms of the absolute skin friction at the top and lower plates, respectively. Moreover, we evaluate the heat transfer rate difference percentage between the nanofluid with hybrid nanofluid and ternary hybrid nanofluid at the upper and lower plates in Table 7 and Table 8, respectively. The absolute skin friction of the ternary hybrid nanofluid is seen to be approximately 5% higher than that of the nanofluid at both plates. Additionally, the rate of heat transmission of the ternary hybrid nanofluid is increased by 1.18% at the bottom plate and 4.33% at the upper plate. Observations indicate that the heat transmission rate of the ternary hybrid nanofluid is higher at the upper plate compared to the lower plate.

Table 5
Comparsion of Skin friction Coefficient for lower plate

ϕ_1	Cu Nanofluid $-Re_x^{1/2}C_{f_1}$	ϕ_2	$Cu-Al_2O_3$ Hybrid Nanofluid $-Re_x^{1/2}C_{f_1}$	Change in Percentage	ϕ_3	$Cu-Al_2O_3-TiO_2$ Ternary Hybrid Nanofluid $-Re_x^{1/2}C_{f_1}$	Change in Percentage
0.01	3.0439	0.01	3.1222	2.57%	0.01	3.2027	5.22%
0.05	3.4157		3.5016	2.51%		3.5896	5.09%
0.1	3.9495		4.0468	2.46%		4.1459	4.97%

Table 6
Comparsion of Skin friction Coefficient for upper plate

ϕ_1	Cu Nanofluid $-Re_x^{1/2}C_{f_2}$	ϕ_2	$Cu-Al_2O_3$ Hybrid Nanofluid $-Re_x^{1/2}C_{f_1}$	Change in Percentage	ϕ_3	$Cu-Al_2O_3-TiO_2$ Ternary Hybrid Nanofluid $-Re_x^{1/2}C_{f_2}$	Change in Percentage
0.01	2.1459	0.01	2.2010	2.56%	0.01	2.2578	5.21%
0.05	2.4026		2.4632	2.52%		2.5254	5.11%
0.1	2.7726		2.8414	2.48%		2.9117	5.02%

Table 7
Comparsion of Local Nusselt number for lower plate

ϕ_1	Cu Nanofluid $-Re_x^{-1/2}Nu_{x_1}$	ϕ_2	$Cu-Al_2O_3$ Hybrid Nanofluid $-Re_x^{-1/2}Nu_{x_1}$	Change in Percentage	ϕ_3	$Cu-Al_2O_3-TiO_2$ Ternary Hybrid Nanofluid $-Re_x^{-1/2}Nu_{x_1}$	Change in Percentage
0.01	3.3136	0.01	3.3348	0.64%	0.01	3.3528	1.18%
0.05	3.4081		3.4328	0.72%		3.4533	1.33%
0.1	3.5418		3.5714	0.84%		3.5950	1.50%

Table 8
Comparsion of Local Nusselt number for upper plate

ϕ_1	Cu Nanofluid $-Re_x^{-1/2}Nu_{x_2}$	ϕ_2	$Cu-Al_2O_3$ Hybrid Nanofluid $-Re_x^{-1/2}Nu_{x_1}$	Change in Percentage	ϕ_3	$Cu-Al_2O_3-TiO_2$ Ternary Hybrid Nanofluid $-Re_x^{-1/2}Nu_{x_2}$	Change in Percentage
0.01	1.2253	0.01	1.2536	2.31%	0.01	1.2784	4.33%
0.05	1.3444		1.3759	2.34%		1.4029	4.35%
0.1	1.5072		1.5431	2.38%		1.5729	4.35%

5. Conclusions

The present study is a comprehensive examination of the impact of thermal radiation on the squeezing flow of a ternary hybrid nanofluid with magnetic field effect between two Parallel Plates, when a heat source/sink is present inside a porous medium. The analysis also takes into account the flow characteristics and their impact on the velocity $f'(\eta)$ and temperature $\theta(\eta)$ profiles, skin friction coefficients, and Nusselt number. The main results of the ongoing study are summarized below:

i. The velocity profile $f'(\eta)$ shows a decrease in pattern when the parameters S and λ on the upper plate and Da on the lower plate are increased. Conversely, it displays an increasing pattern with higher values of Sq and λ on the lower plate, as well as Da on the upper plate.
ii. The velocity $f'(\eta)$ of the ternary hybrid nanofluid decreases as the magnetic parameter increases near the lower plate, but increases near the upper plate.
iii. The temperature $\theta(\eta)$ decreases as the values of R and Sq increase, whereas it increases with the increase of δ, Q, S and λ.
iv. The absolute skin friction of the ternary hybrid nanofluid is seen to be approximately 5% higher than that of the regular nanofluid at both lower and upper plates.
v. The ternary hybrid nanofluid demonstrates superior heat transfer efficiency compared to the hybrid nanofluid, while the hybrid nanofluid displays higher heat transfer efficiency than standard nanofluids.
vi. The heat transmission rate of the ternary hybrid nanofluid is higher at the upper plate compared to the lower plate.

The future potential of ternary hybrid nanofluids, which consist of copper (Cu), aluminum oxide (Al_2O_3), and titanium dioxide (TiO_2), is significant in multiple scientific and technical fields. Ternary hybrid nanofluids provide the possibility of greatly enhancing heat transfer efficiency in various applications, such as radiators, heat exchangers and cooling devices. Improved heat transfer properties might be beneficial for use in geothermal power extraction, solar energy systems and high-temperature operations.

Acknowledgement
We express our gratitude to the Reviewers for dedicating their valuable time and exerting the necessary effort to thoroughly evaluate the research paper. We deeply value your insightful comments and recommendations, since they have significantly contributed to enhancing the quality of the manuscript.

References

[1] Choi, S. U. S., and Jeffrey A. Eastman. *Enhancing thermal conductivity of fluids with nanoparticles*. No. ANL/MSD/CP-84938; CONF-951135-29. Argonne National Lab.(ANL), Argonne, IL (United States), 1995.

[2] Raees, Ammarah, Hang Xu, and Shi-Jun Liao. "Unsteady mixed nano-bioconvection flow in a horizontal channel with its upper plate expanding or contracting." *International Journal of Heat and Mass Transfer* 86 (2015): 174-182. https://doi.org/10.1016/j.ijheatmasstransfer.2015.03.003

[3] Hayat, T., Taseer Muhammad, A. Qayyum, A. Alsaedi, and M. Mustafa. "On squeezing flow of nanofluid in the presence of magnetic field effects." *Journal of Molecular Liquids* 213 (2016): 179-185. https://doi.org/10.1016/j.molliq.2015.11.003

[4] Hayat, Tasawar, Rai Sajjad, Ahmed Alsaedi, Taseer Muhammad, and Rahmat Ellahi. "On squeezed flow of couple stress nanofluid between two parallel plates." *Results in Physics* 7 (2017): 553-561. https://doi.org/10.1016/j.rinp.2016.12.038

[5] Salehi, Sajad, Amin Nori, Kh Hosseinzadeh, and D. D. Ganji. "Hydrothermal analysis of MHD squeezing mixture fluid suspended by hybrid nanoparticles between two parallel plates." *Case Studies in Thermal Engineering* 21 (2020): 100650. https://doi.org/10.1016/j.csite.2020.100650

[6] Acharya, Nilankush. "On the flow patterns and thermal behaviour of hybrid nanofluid flow inside a microchannel in presence of radiative solar energy." *Journal of Thermal Analysis and Calorimetry* 141, no. 4 (2020): 1425-1442. https://doi.org/10.1007/s10973-019-09111-w

[7] Acharya, Nilankush, Raju Bag, and Prabir Kumar Kundu. "Unsteady bioconvective squeezing flow with higher-order chemical reaction and second-order slip effects." *Heat Transfer* 50, no. 6 (2021): 5538-5562. https://doi.org/10.1002/htj.22137

[8] Islam, Saeed, Arshad Khan, Wejdan Deebani, Ebenezer Bonyah, Nasser Aedh Alreshidi, and Zahir Shah. "Influences of Hall current and radiation on MHD micropolar non-Newtonian hybrid nanofluid flow between two surfaces." *AIP Advances* 10, no. 5 (2020). https://doi.org/10.1063/1.5145298

[9] Ikram, Muhammad Danish, Muhammad Imran Asjad, Ali Akgül, and Dumitru Baleanu. "Effects of hybrid nanofluid on novel fractional model of heat transfer flow between two parallel plates." *Alexandria Engineering Journal* 60, no. 4 (2021): 3593-3604. https://doi.org/10.1016/j.aej.2021.01.054

[10] Khashi'ie, Najiyah Safwa, Iskandar Waini, Norihan Md Arifin, and Ioan Pop. "Unsteady squeezing flow of Cu-Al_2O_3/water hybrid nanofluid in a horizontal channel with magnetic field." *Scientific Reports* 11, no. 1 (2021): 14128. https://doi.org/10.1038/s41598-021-93644-4

[11] Yaseen, Moh, Sawan Kumar Rawat, Anum Shafiq, Manoj Kumar, and Kamsing Nonlaopon. "Analysis of heat transfer of mono and hybrid nanofluid flow between two parallel plates in a Darcy porous medium with thermal radiation and heat generation/absorption." *Symmetry* 14, no. 9 (2022): 1943. https://doi.org/10.3390/sym14091943

[12] Rostami, H. Talebi, M. Fallah Najafabadi, Kh Hosseinzadeh, and D. D. Ganji. "Investigation of mixture-based dusty hybrid nanofluid flow in porous media affected by magnetic field using RBF method." *International Journal of Ambient Energy* 43, no. 1 (2022): 6425-6435. https://doi.org/10.1080/01430750.2021.2023041

[13] Rauf, Abdul, Faisal, Nehad Ali Shah, and Thongchai Botmart. "Hall current and morphological effects on MHD micropolar non-Newtonian tri-hybrid nanofluid flow between two parallel surfaces." *Scientific Reports* 12, no. 1 (2022): 16608. https://doi.org/10.1038/s41598-022-19625-3

[14] Waini, Iskandar, Anuar Ishak, and Ioan Pop. "Radiative and magnetohydrodynamic micropolar hybrid nanofluid flow over a shrinking sheet with Joule heating and viscous dissipation effects." *Neural Computing and Applications* 34, no. 5 (2022): 3783-3794. https://doi.org/10.1007/s00521-021-06640-0

[15] Famakinwa, O. A., O. K. Koriko, and K. S. Adegbie. "Effects of viscous dissipation and thermal radiation on time dependent incompressible squeezing flow of CuO− Al_2O_3/water hybrid nanofluid between two parallel plates with variable viscosity." *Journal of Computational Mathematics and Data Science* 5 (2022): 100062. https://doi.org/10.1016/j.jcmds.2022.100062

[16] Bilal, Muhammad, A. El-Sayed Ahmed, Rami Ahmad El-Nabulsi, N. Ameer Ahammad, Khalid Abdulkhaliq M. Alharbi, Mohamed Abdelghany Elkotb, Waranont Anukool, and Zedan A. S. A. "Numerical analysis of an unsteady, electroviscous, ternary hybrid nanofluid flow with chemical reaction and activation energy across parallel plates." *Micromachines* 13, no. 6 (2022): 874. https://doi.org/10.3390/mi13060874

[17] Hanif, Hanifa, Wasim Jamshed, Mohamed R. Eid, Rabha W. Ibrahim, Sharidan Shafie, Aeshah A. Raezah, and Sayed M. El Din. "Numerical Crank-Nicolson methodology analysis for hybridity aluminium alloy nanofluid flowing based-water via stretchable horizontal plate with thermal resistive effect." *Case Studies in Thermal Engineering* 42 (2023): 102707. https://doi.org/10.1016/j.csite.2023.102707

[18] Noor, Nur Azlina Mat, and Sharidan Shafie. "Magnetohydrodynamics squeeze flow of sodium alginate-based Jeffrey hybrid nanofluid with heat sink or source." *Case Studies in Thermal Engineering* 49 (2023): 103303. https://doi.org/10.1016/j.csite.2023.103303

[19] Ullah, Asad, Nahid Fatima, Khalid Abdulkhaliq M. Alharbi, Samia Elattar, and Waris Khan. "A numerical analysis of the hybrid nanofluid (Ag+ TiO_2+ water) flow in the presence of heat and radiation fluxes." *Energies* 16, no. 3 (2023): 1220. https://doi.org/10.3390/en16031220

[20] Roy, Nepal Chandra, and Ioan Pop. "Analytical investigation of transient free convection and heat transfer of a hybrid nanofluid between two vertical parallel plates." *Physics of Fluids* 34, no. 7 (2022). https://doi.org/10.1063/5.0096694

[21] Jayavel, Prakash, Ramesh Katta, and Ram Kishun Lodhi. "Numerical analysis of electromagnetic squeezing flow through a parallel porous medium plate with impact of suction/injection." *Waves in Random and Complex Media* (2022): 1-24. https://doi.org/10.1080/17455030.2022.2088890

[22] Bhaskar, Kajal, Kalpna Sharma, and Khushbu Bhaskar. "MHD Squeezed Radiative Flow of Casson Hybrid Nanofluid Between Parallel Plates with Joule Heating." *International Journal of Applied and Computational Mathematics* 10, no. 2 (2024): 80. https://doi.org/10.1007/s40819-024-01720-w

[23] Maiti, Hiranmoy, and Swati Mukhopadhyay. "Squeezing unsteady nanofluid flow among two parallel plates with first-order chemical reaction and velocity slip." *Heat Transfer* 53, no. 4 (2024): 1790-1815. https://doi.org/10.1002/htj.23015

[24] Madit, Benjamin Matur, Jackson K. Kwanza, and Phineas Roy Kiogora. "Hydromagnetic Squeezing Nanofluid Flow between Two Vertical Plates in Presence of a Chemical Reaction." *Journal of Applied Mathematics and Physics* 12, no. 1 (2024): 126-146. https://doi.org/10.4236/jamp.2024.121011

[25] Khashi'ie, Najiyah Safwa, Norihan Md Arifin, Ezad Hafidz Hafidzuddin, and Nadihah Wahi. "Dual stratified nanofluid flow past a permeable shrinking/stretching sheet using a non-Fourier energy model." *Applied Sciences* 9, no. 10 (2019): 2124. https://doi.org/10.3390/app9102124

[26] Khashi'ie, Najiyah Safwa, Ezad Hafidz Hafidzuddin, Norihan Md Arifin, and Nadihah Wahi. "Stagnation point flow of hybrid nanofluid over a permeable vertical stretching/shrinking cylinder with thermal stratification effect." *CFD Letters* 12, no. 2 (2020): 80-94.

[27] Nath, Rupam Shankar, and Rudra Kanta Deka. "Theoretical study of thermal and mass stratification effects on MHD nanofluid past an exponentially accelerated vertical plate in a porous medium in presence of heat source, thermal radiation and chemical reaction." *International Journal of Applied and Computational Mathematics* 10, no. 2 (2024): 92. https://doi.org/10.1007/s40819-024-01721-9

[28] Nath, Rupam Shankar, and Rudra Kanta Deka. "Thermal and mass stratification effects on MHD nanofluid past an exponentially accelerated vertical plate through a porous medium with thermal radiation and heat source." *International Journal of Modern Physics B* (2024): 2550045. https://doi.org/10.1142/S0217979225500456

[29] Nath, Rupam Shankar, and Rudra Kanta Deka. "Thermal and mass stratification effects on unsteady parabolic flow past an infinite vertical plate with exponential decaying temperature and variable mass diffusion in porous medium." *ZAMM-Journal of Applied Mathematics and Mechanics/Zeitschrift für Angewandte Mathematik und Mechanik* (2024): e202300475. https://doi.org/10.1002/zamm.202300475

[30] Nath, Rupam Shankar, and Rudra Kanta Deka. "A Numerical Study on the MHD Ternary Hybrid Nanofluid (Cu-Al_2O_3-TiO_2/H_2O) in presence of Thermal Stratification and Radiation across a Vertically Stretching Cylinder in a Porous Medium." *East European Journal of Physics* 1 (2024): 232-242. https://doi.org/10.26565/2312-4334-2024-1-19

[31] Nath, Rupam Shankar, and Rudra Kanta Deka. "A Numerical Investigation of the MHD Ternary Hybrid Nanofluid (Cu-Al_2O_3-TiO_2/H_2O) Past a Vertically Stretching Cylinder in a Porous Medium with Thermal Stratification." *Journal of Advanced Research in Fluid Mechanics and Thermal Sciences* 116, no. 1 (2024): 78-96. https://doi.org/10.37934/arfmts.116.1.7896

[32] Ullah, Hakeem, Muhammad Shoaib, Ajed Akbar, Muhammad Asif Zahoor Raja, Saeed Islam, and Kottakkaran Sooppy Nisar. "Neuro-computing for hall current and MHD effects on the flow of micro-polar nano-fluid between two parallel rotating plates." *Arabian Journal for Science and Engineering* 47, no. 12 (2022): 16371-16391. https://doi.org/10.1007/s13369-022-06925-z

[33] Ullah, Hakeem, Imran Khan, Hussain AlSalman, Saeed Islam, Muhammad Asif Zahoor Raja, Muhammad Shoaib, Abdu Gumaei et al. "Levenberg-Marquardt backpropagation for numerical treatment of micropolar flow in a porous channel with mass injection." Complexity 2021, no. 1 (2021): 5337589. https://doi.org/10.1155/2021/5337589

[34] Shoaib, Muhammad, Rafaqat Ali Khan, Hakeem Ullah, Kottakkaran Sooppy Nisar, Muhammad Asif Zahoor Raja, Saeed Islam, Bassem F. Felemban, and I. S. Yahia. "Heat transfer impacts on Maxwell nanofluid flow over a vertical moving surface with MHD using stochastic numerical technique via artificial neural networks." *Coatings* 11, no. 12 (2021): 1483. https://doi.org/10.3390/coatings11121483

[35] Akbar, Ajed, Hakeem Ullah, Muhammad Asif Zahoor Raja, Kottakkaran Sooppy Nisar, Saeed Islam, and Muhammad Shoaib. "A design of neural networks to study mhd and heat transfer in two phase model of nano-fluid flow in the presence of thermal radiation." *Waves in Random and Complex Media* (2022): 1-24. https://doi.org/10.1080/17455030.2022.2152905

[36] Akbar, Ajed, Hakeem Ullah, Kottakkaran Sooppy Nisar, Muhammad Asif Zahoor Raja, Muhammad Shoaib, and Saeed Islam. "Intelligent computing paradigm for the Buongiorno model of nanofluid flow with partial slip and MHD effects over a rotating disk." *ZAMM-Journal of Applied Mathematics and Mechanics/Zeitschrift für Angewandte Mathematik und Mechanik* 103, no. 1 (2023): e202200141. https://doi.org/10.1002/zamm.202200141

[37] Ullah, Hakeem, Saeed Islam, and Mehreen Fiza. "Analytical solution for three-dimensional problem of condensation film on inclined rotating disk by extended optimal homotopy asymptotic method." *Iranian Journal of Science and Technology, Transactions of Mechanical Engineering* 40 (2016): 265-273. https://doi.org/10.1007/s40997-016-0030-8

[38] Fiza, M., Hakeem Ullah, and S. Islam. "Three-dimensional mhd rotating flow of viscoelastic nanofluid in porous medium between parallel plates." *Journal of Porous Media* 23, no. 7 (2020). https://doi.org/10.1615/JPorMedia.2020027478

[39] Elfiano, Eddy, Nik Mohd Izual Nik Ibrahim, and Muhammad Khairul Anuar Mohamed. "Mixed Convection Boundary Layer Flow on A Vertical Flat Plate in Al_2O_3-Ag/Water Hybrid Nanofluid with Viscous Dissipation Effects." *Journal of Advanced Research in Numerical Heat Transfer* 22, no. 1 (2024): 1-13. https://doi.org/10.37934/arnht.22.1.113

[40] Annapurna, T., K. S. R. Sridhar, and M. Karuna Prasad. "Effect of Different Shapes of Nanoparticles on Mixed Convective Nanofluid Flow in a Darcy-Forchhiemer Porous Medium." *CFD Letters* 16, no. 12 (2024): 38-58. https://doi.org/10.37934/cfdl.16.12.3858

[41] Hale, Nicholas, and D. Moore. "A sixth-order extension to the MATLAB package bvp4c of J. Kierzenka and L. Shampine." *University of Oxford* (2008).

[42] Rosseland, Svein. *Astrophysik: Auf Atomtheoretischer Grundlage*. Springer-Verlag, 1931. https://doi.org/10.1007/978-3-662-26679-3

[43] Das, S., and R. N. Jana. "Natural convective magneto-nanofluid flow and radiative heat transfer past a moving vertical plate." *Alexandria Engineering Journal* 54, no. 1 (2015): 55-64. https://doi.org/10.1016/j.aej.2015.01.001

[44] Waini, Iskandar, Anuar Ishak, and Ioan Pop. "Mixed convection flow over an exponentially stretching/shrinking vertical surface in a hybrid nanofluid." *Alexandria Engineering Journal* 59, no. 3 (2020): 1881-1891. https://doi.org/10.1016/j.aej.2020.05.030